MJFAS
Malaysian Journal of Fundamental and Applied Sciences

1972-2022
KERANA TUHAN UNTUK MANUSIA



RESEARCH ARTICLE

# Numerical Simulation of a Three-dimensional Subsea Cable with Buoyancy Module

**Nur Adlin Lina Normisyidi[a]*, Ahmad Razin Zainal Abidin[a], and Yeak Su Hoe[b]**

[a] Department of Structure and Material, School of Civil Engineering, Faculty of Engineering, Universiti Teknologi Malaysia, 81310 UTM Johor Bahru, Johor, Malaysia; [b]Department of Mathematical Sciences, Faculty of Science, Universiti Teknologi Malaysia, 81310 UTM Johor Bahru, Johor, Malaysia

**Abstract** Extreme formation of slacks and entanglement with risers induced from a small diameter and high structural flexibility of subsea cable is often being a huge challenge in subsea cable installation. In many cases, the cable is prone to breaking, bending, or twisting due to the rough and dynamic underwater condition. One of the alternatives is the use of buoyancy module to facilitate the cable installation and to reduce cable tension and false slacks. This paper proposes reliable three-dimensional mathematical model and simulation to specifically investigate the behaviour of subsea cable with buoyancy module during laying operation. A finite difference method (FDM) and optimization algorithm is used to discretize the formulation and simulate this type of subsea cable problem concerning on the tensional analysis. The methodology is specifically designed to allow cable configuration to be changed over time as a result from the buoyancy module. The viability subsea cable configuration with existence of buoyancy module has been showed successfully reduce the cable tension especially at the hang-off section.

**Keywords**: Subsea cable, Buoyancy module, Dynamic model

## Introduction

The subsea cable laying process is still one of the risky and challenging issue faced by engineer due to many uncertainties in deep water arise during the operation. The cable ship tends to move backward and forward due to unstable ocean current and wave. On that account, it causes the subsea cable to form slacks, a phenomenon which the cable configuration curves tend to be fatter when the cable touches the seabed and this lead to cable breaking, bending or twisting [1]. Due to the formation of false slack, it will increase the possibility of the cable being laid too long along the planned route. Installing any type of subsea cable with high slacks can resulting in more subsea cable usage than necessary, hence increasing the cost of the operation, while laying a subsea cable with high tension or too low slack could result in damaging kink at the touchdown of the seabed. The analysis of subsea cable tension and configuration in deepwater plays an important role in the cable system design. Once the investigation about the mechanics and behaviour of subsea cable available, it may mitigate the possible formation of slacks during the laying operation as well as improve operation efficiently. Therefore, the tension analysis of subsea cable has been a great topic to be explore for researcher since the past few decades.

Most researchers, but only few of them may use some special cases to get cable position information [2-4]. In addition, in many cases, the use of buoyancy module was ignored in the model formulation as to preserve the simplicity and easy installation of the subsea cable. However, several researches have claimed that this kind of model is very sensitive to fatigue and excessive structural stresses may cause a large hang-off loads at the top tension when the cable is being submerged in deeper ocean [5, 6].

***For correspondence:**
adlinlina40@yahoo.com

**Received:** 10 March 2022
**Accepted:** 31 Oct. 2022

Generally, it is considered as a crucial challenge for subsea cable that must withstand high tension transferred from free hanging cable configuration [7-9].

One of the alternatives is installing a buoyancy module to the specific region of a free-hanging cable, forming a lazy-wave configuration in order to facilitate the cable installation and to create a gentler configuration where arc bend and sag bend parts are made within the configuration [10]. This buoyancy module generates an upward buoyancy force to eliminate partial tension, thus it is employed as a viable solution in deepwater application. Kim and Kim [10] model suspended section of lazy-wave configuration as three individual catenaries, each catenary has individual origin and local coordinate. Comprehensive researches on mechanics and installation of lazy-wave subsea cable have been done by [5, 7, 11, 12] but they are all based on 2D static model. However, with subsea cable installation generally taking place in ever-increasing water depths and increasing in subsea cable length, the influence of dynamic factors on the subsea cable has become increasingly apparent [13]. Although the 2D formulation is sufficient to predict the dynamics in the reference plane of static equilibrium, yet it certainly would be a short approximation in the analysis. Although the 2D formulation is sufficient to predict the dynamics in the reference plane of static equilibrium, yet it certainly would be a short approximation in the analysis. So, 3D formulation is required especially when investigating the subsea cable configuration under specific conditions (e.g. subjected to vessel offsets or ocean wave-current loads).

Some researches on the dynamic response on the lazy-wave cable have been conducted. Li and Nguyen [14] used catenary theory without considering the effect of bending stiffness, therefore the mechanical behaviours of lazy-wave were not accurate enough and ocean current cannot be taken into account. Furthermore, Oh, Jung [15] conducted simulation-based design process to find the optimal shape of lazy-wave cable. Wang, Duan [11] conducted a 2D dynamic study on lazy-wave riser by investigating the influences of tangential and normal excitation on the riser's dynamic response. In addition, there is a significant change of inclination angle and curvature section of arch bend and sag bend on lazy-wave cable configuration. Therefore, the mechanical behaviors cannot be calculated using traditional analytical methods or either depending on commercial analysis technique such finite element software. Ai, Xu [16] studied the stress and fatigue damage along the lazy-wave cable with the different distribution of buoyancy module and Cheng, Tang [17] presents a time-domain numerical scheme to study the influences of buoyancy segment length on the subsea cable's dynamic behaviour.

Appropriate formulation of the theoretical model and the use of an efficient solution method are the important issues that required in the dynamic analysis. The most popular proposed method for subsea cable problem is finite element method (FEM). FEM not the only numerical method that can be used to explore the dynamic behaviour of subsea cable. Finite difference method (FDM) can be equally efficient for solving the dynamic problem of catenary shaped structure [18]. However, the couple discretization that required in time and space create the difficulties on the use of FDM. Nevertheless, this problem was properly address by Hoffman [19] and the method introduced is Keller Box Finite Difference numerical scheme, known as the Box method. Ablow and Schechter [20] first employed the Box method in cable dynamics system and expended by Milinazzo, Wilkie [21] to produce more efficient and stable method. The same method was successfully applied to the analysis of lazy-wave cable by Chatjigeorgiou [22] and Wang, Duan [11]. Thus, the method is properly employed herein for the solution of the 3D dynamic subsea cable problem.

In this paper, a three-dimensional dynamic subsea cable model based on Euler-Bernoulli beam theory with initial conditions and boundary conditions is proposed. In order to reduce the formation of false slack during laying operation, particular attention is paid on the tensional analysis of subsea cable for both subsea cable model under the same environmental condition and the dynamic characteristic. The numerical results are obtained by using MATLAb language program based on Keller box finite difference scheme in order to investigate the cable configuration, tension distribution, and bending moment. The result is proved to be reasonable and practicable. It can provide a significant and basic references for the tensional analysis of deepwater subsea cable.

## Theoretical Model

This section focuses on developing a mathematical model of the subsea cable problem. The dynamic equations which form the basis of the mathematical model of subsea cable are derived using Euler-Bernoulli beam model with initial conditions and boundary conditions. There are two types of cable configuration studied, free-hanging subsea cable (subsea cable without buoyancy module) and lazy-wave subsea cable (subsea cable with buoyancy module). A lazy-wave subsea cable is a special and advanced free-hanging cable with a segment of its length equipped with buoyancy modules.

The following assumption are considered in this study: (1) Due to the relatively smaller rotational inertia terms in comparison with the bending stiffness terms, the analysis is conducted in the 3D plane without considering torsion. (2) The cable is assumed to be non-extensible Euler-Bernoulli beam since the cable material is isotropic and always in elastic state. (3) The cable is assumed to be pinned at the horizontal and rigid seabed. Analyzing the cable is limited to the portions that are fully immersed, no portion above the seawater level is considered.

## General configuration of free-hanging subsea cable

Free-hanging configuration is known for the model of the subsea cable without buoyancy module. The geometry of this free-hanging configuration is primary based on the catenary equation which can be described as a hyperbolic cosine function as in Equation 1 and it can be illustrated as in Figure 1.

$$y = a(cosh\frac{x}{a} - 1) \tag{1}$$

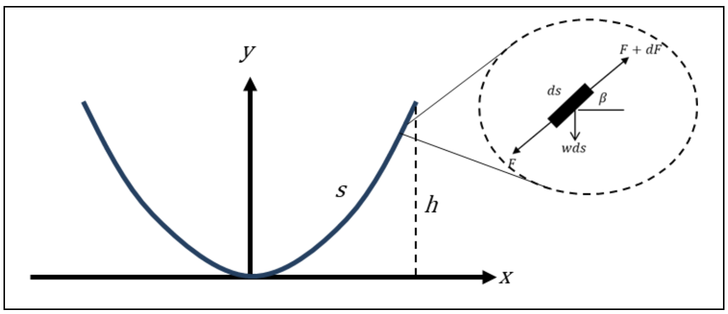


**Figure 1.** Representation of the general shape of catenary.

In Equation 1, $a$ denoted as the curvature radius at the origin where the curvatures can be defined as follows in Equation 2. However,

$$k = \frac{1}{a\cosh^2\frac{x}{a}} \tag{2}$$

Based on the Figure 1, the following relationship can be derived by horizontal and vertical force equilibrium and they can be used to determine the initial coordinate of the free-hanging cable in the water where $s$ is the arc length of cable from origin, $h$ is the water depth and $\beta$ is the inclination angle.

$$s = a\,sinh\left(\frac{x}{a}\right) \tag{3}$$

$$\beta = \tan^{-1}\left(\frac{s}{a}\right) \tag{4}$$

In order to solve for $x$, it is necessary to find the value of $a$ which models the catenary cable shape. To find the $a$ value, we fixed the value of $s$ and $h$ then divide both Equation 1 and 3 by $a$, square both of them and subtract them. Using hyperbolic identity

$$\cosh^2 t - \sinh^2 t = 1 \tag{5}$$

We get

$$\left(\frac{h+a}{a}\right)^2 - \left(\frac{s}{a}\right)^2 = 1 \tag{6}$$

By solving Equation 6, we get the value of $a$, and plugging $a$ into Equation 1 we can solve for $x$.

During the practical installation of free-hanging subsea cable (as shown in Figure 2), the cable is laid on the seabed in which the last point of cable touches the seabed is known as touch down point, TDP. The TDP will be initial point as to measure the length of subsea cable until it laid up to the point of cable hanging at the floating vessel. Parameter $s$ (arc length) is introduced to denote the length of subsea cable. Then, $h$ is the depth of water and $l$ is the length from origin O until the position of vessel in $x$-axis.

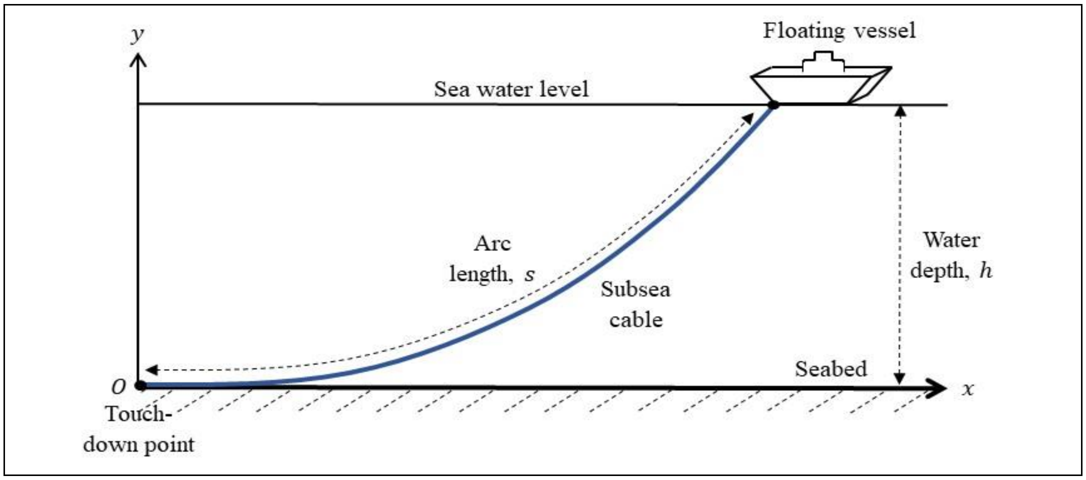


**Figure 2.** Schematic of 2D subsea cable in free-hanging configuration.

## General configuration of lazy-wave subsea cable

A lazy-wave configuration is special and advanced free-hanging cable that equipped with buoyancy modules. The buoyancy module was normally installed to the middle section of a free-hanging configuration, creating an upward buoyancy force forming a lazy-wave configuration [5]. The distributed downward buoyancy force is lesser than the upward gravity force, resulting an arch bend [11]. Kim and Kim [10] have provided a complete calculation procedure for determine the configuration/catenary equations and ranges of each catenary sections of lazy-wave configuration.

Same as free-hanging cable, the bottom end point $O$ known as TDP which last point of cable touches the seabed while the top end point E is attached to the floating vessel. Both entire model of free-hanging and lazy-wave are established in global coordinated system $(x, y, z)$. The lazy-wave configuration consists of three individual catenary sections (as shown in Figure 3): touchdown catenary O-A, buoyancy catenary A-B-C is where the buoyancy modules are installed, and hang-off catenary C-D-E is where the cable hung by the floating vessel at the hang-off point E. The arch bend at point B is the peak of the arch bend while the point D is the lowest point of sag bend.

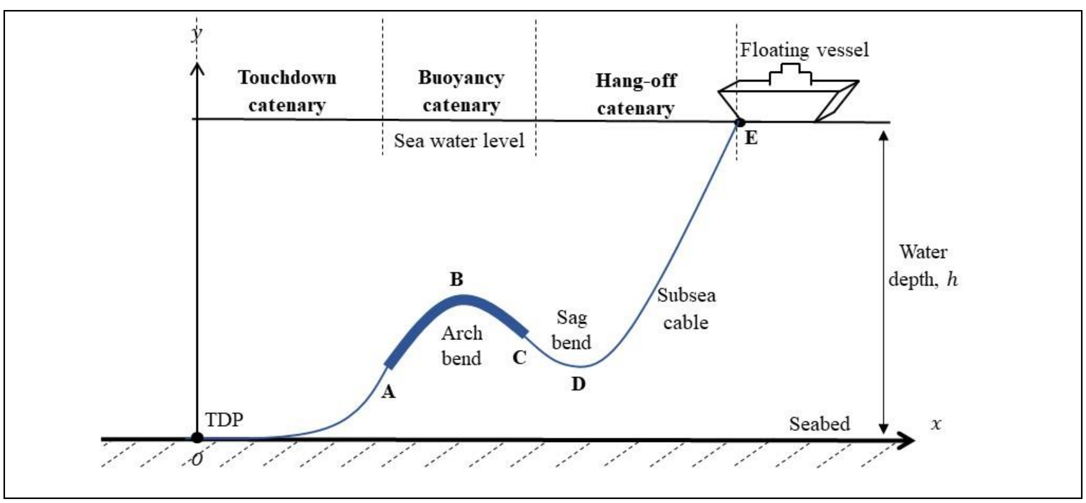


**Figure 3.** Schematic of 2D subsea cable in lazy-wave configuration.

## Governing equations for free-hanging subsea cable model

The nonlinear Euler-Bernoulli beam theory is properly adopted to dynamic model of subsea cable as it can simulate the large deformation dynamic behaviour successfully [23]. The 3D dynamic governing equations of the subsea cable is governed by ten partial differential equations. These equations are provided in the following without further details on the derivation work which can be referred to the works of [11] and [23].

$$m_r \frac{\partial u}{\partial t} + m_r \left( w \frac{\partial \theta}{\partial t} - v \frac{\partial \phi}{\partial t} \cos\theta \right) = \frac{\partial T}{\partial s} + S_b \Omega_n - S_n \Omega_b$$
$$-w_r \sin\phi \cos\theta - \frac{1}{2}\pi \rho d_0 C_{dt}(v_{tr})|v_{tr}| \left(1 + \frac{T}{EA}\right)^{\frac{1}{2}} \tag{5}$$

$$m_r \frac{\partial v}{\partial t} + m_r \left( u \frac{\partial \phi}{\partial t} cos\,\theta + w \frac{\partial \phi}{\partial t} sin\,\theta \right) = \frac{\partial S_n}{\partial s} + T\Omega_b + S_b \Omega_b \tan\theta - w_r \cos\phi$$
$$-m_{ra} \frac{\partial v_{nr}}{\partial t} - \frac{1}{2}\rho d_0 C_{dn}(v_{nr})|(v_{nr})^2 + (v_{br})^2|^{\frac{1}{2}} \left(1 + \frac{T}{EA}\right)^{\frac{1}{2}} \tag{6}$$

$$m_r \frac{\partial w}{\partial t} - m_r \left( v \frac{\partial \phi}{\partial t} \sin\theta + u \frac{\partial \theta}{\partial t} \right) = \frac{\partial S_b}{\partial s} - S_n \Omega_b \tan\theta - T\Omega_2 - w_r \sin\phi \sin\theta$$
$$-m_{ra} \frac{\partial v_{br}}{\partial t} + -\frac{1}{2}\rho d_0 C_{db}(v_{br})|(v_{nr})^2 + (v_{br})^2|^{\frac{1}{2}} \left(1 + \frac{T}{EA}\right)^{\frac{1}{2}} \tag{7}$$

$$\frac{1}{EA}\frac{\partial T}{\partial t} = \frac{\partial u}{\partial s} + w\Omega_n - v\Omega_b \tag{8}$$

$$\left(1 + \frac{T}{EA}\right)\frac{\partial \phi}{\partial t}\cos\theta = \frac{\partial v}{\partial s} + u\Omega_b + w\Omega_b \tan\theta \tag{9}$$

$$-\left(1 + \frac{T}{EA}\right)\frac{\partial \theta}{\partial t} = \frac{\partial w}{\partial s} - v\Omega_b \tan\theta - u\Omega_n \tag{10}$$

$$EI\frac{\partial \Omega_n}{\partial s} = EI\Omega_b^2 \tan\theta + (1+e)^3 S_b \tag{11}$$

$$EI\frac{\partial \Omega_b}{\partial s} = EI\Omega_n\Omega_b \tan\theta - (1+e)^3 S_n \tag{12}$$

$$\frac{\partial \theta}{\partial s} = \Omega_n \tag{13}$$

$$\frac{\partial \phi}{\partial s}\cos\theta = \Omega_b \tag{14}$$

where the model of free-hanging subsea cable having the following geometrical and physical properties: outer diameter $d_o$, submerged weight $w_r$, mass $m_r$, added mass $m_{ra}$, bending stiffness $EI$, elastic stiffness $EA$, and eulerian angles $\phi$ and $\theta$. $\phi$ is eulerian angle formed between the tangent of the cable and horizontal reference plane while $\theta$ is eulerian angle in the out-of-plane direction. The moments $M_n$ and $M_b$ are related with the corresponding curvatures $\Omega_n$ and $\Omega_b$ according to $M_j = E\Omega_j$, for $j = n, b$. $v_{tr}, v_{nr}$, and $v_{br}$ is the relative velocity at tangential direction, normal direction, and binormal direction respectively. When the steady ocean current is presented, the relative velocities can be written as $v_{tr} = u - U_t$, $v_{nr} = v - U_n$, and $v_{br} = w - U_b$, where $U_t, U_n$ and $U_b$ are components of steady current.

## Governing equations for lazy-wave subsea cable model

The 3D dynamic equations for lazy-wave subsea cable model are derived based on Equation 5 – Equation 14. The governing equations for touchdown catenary and hang-off catenary sections are same as Equations 5 – 14 since the cable shape for both catenary sections are referring to the free-hanging setting. However, buoyancy catenary section is covered by many pieces of buoyancy modules which provide buoyancy force. Using equivalent parameters, the governing equations of buoyancy catenary section like Equation 5 – 14 are as follows:

$$m_b \frac{\partial u}{\partial t} + m_b \left( w \frac{\partial \theta}{\partial t} - v \frac{\partial \phi}{\partial t} \cos\theta \right) = \frac{\partial T}{\partial s} + S_b \Omega_n - S_n \Omega_b$$
$$-w_b \sin\phi \cos\theta - \frac{1}{2} \pi \rho d_0 C_{dt} (v_{tr}) |v_{tr}| \left(1 + \frac{T}{EA}\right)^{\frac{1}{2}} \tag{15}$$

$$m_b \frac{\partial v}{\partial t} + m_b \left( u \frac{\partial \phi}{\partial t} cos\,\theta + w \frac{\partial \phi}{\partial t} sin\,\theta \right) = \frac{\partial S_n}{\partial s} + T\Omega_b + S_b \Omega_b \tan\theta - w_b \cos\phi$$
$$-m_{ba} \frac{\partial v_{nr}}{\partial t} - \frac{1}{2} \rho d_0 C_{dn} (v_{nr}) |(v_{nr})^2 + (v_{br})^2|^{\frac{1}{2}} \left(1 + \frac{T}{EA}\right)^{\frac{1}{2}} \tag{16}$$

$$m_b \frac{\partial w}{\partial t} - m_b \left( v \frac{\partial \phi}{\partial t} \sin\theta + u \frac{\partial \theta}{\partial t} \right) = \frac{\partial S_b}{\partial s} - S_n \Omega_b \tan\theta - T\Omega_2 - w_b \sin\phi \sin\theta$$
$$-m_{ba} \frac{\partial v_{br}}{\partial t} + -\frac{1}{2} \rho d_0 C_{db} (v_{br}) |(v_{nr})^2 + (v_{br})^2|^{\frac{1}{2}} \left(1 + \frac{T}{EA}\right)^{\frac{1}{2}} \tag{17}$$

$$\frac{1}{EA} \frac{\partial T}{\partial t} = \frac{\partial u}{\partial s} + w\Omega_n - v\Omega_b \tag{18}$$

$$\left(1 + \frac{T}{EA}\right) \frac{\partial \phi}{\partial t} \cos\theta = \frac{\partial v}{\partial s} + u\Omega_b + w\Omega_b \tan\theta \tag{19}$$

$$-\left(1 + \frac{T}{EA}\right) \frac{\partial \theta}{\partial t} = \frac{\partial w}{\partial s} - v\Omega_b \tan\theta - u\Omega_n \tag{20}$$

$$EI \frac{\partial \Omega_n}{\partial s} = EI\Omega_b^2 \tan\theta + (1+e)^3 S_b \tag{21}$$

$$EI \frac{\partial \Omega_b}{\partial s} = EI\Omega_n \Omega_b \tan\theta - (1+e)^3 S_n \tag{22}$$

$$\frac{\partial \theta}{\partial s} = \Omega_n \tag{23}$$

$$\frac{\partial \phi}{\partial s} \cos\theta = \Omega_b \tag{24}$$

where $m_b$ is equivalent mass, $m_{ba}$ is equivalent added mass, and $w_b$ is equivalent submerged weight of buoyancy section.

## Boundary conditions

To complete the mathematical model, boundary conditions must be obtained by considering the physical and mechanical laws of the subsea cable. One end of the cable $(s = 0)$ is considered as free boundary which the lower end of the subsea cable (at touch down point) is assumed to fix the point where the cable buries itself in a trench while the other end $(s = L)$ is pinned to a ship. At free boundary, the tension, moment, and shear forces are all zero. At the pinned end, the three velocities $(u, v, w)$ are prescribed, and the moments are set equal zero. Mathematically, these boundary conditions are expressed as follows:

$$T(t,0) = S_n(t,0) = S_b(t,0) = 0 \tag{25}$$
$$EI\Omega_n(t,0) = 0 \tag{26}$$
$$EI\Omega_b(t,0) = 0 \tag{27}$$
$$EI \frac{\partial \Omega_n(t,0)}{\partial s} = 0 \tag{28}$$
$$EI \frac{\partial \Omega_b(t,0)}{\partial s} = 0 \tag{29}$$
$$u(t,L) = U(t) \tag{30}$$
$$v(t,L) = V(t) \tag{31}$$
$$w(t,L) = W(t) \tag{32}$$
$$EI\Omega_n(t,L) = 0 \tag{33}$$
$$EI\Omega_b(t,L) = 0 \tag{34}$$

### Initial conditions

The initial condition of subsea cable is set to the whole mechanical parameters at a static equilibrium position. The static equilibrium position should be calculated initially, and then boundary conditions are adopted to conduct dynamic analysis. The static equilibrium also can be numerically calculated based on the static model simplified from 3D dynamic model (which the time items should be eliminated) and the static 3D boundary conditions. The 3D static boundary conditions are listed as follows:

$$T(0) = T_{TDP} \tag{35}$$
$$S_n(0) = 0 \tag{36}$$
$$S_b(0) = 0 \tag{37}$$
$$EI\Omega_n(0) = 0 \tag{38}$$
$$EI\Omega_b(0) = 0 \tag{39}$$
$$u(L) = 0 \tag{40}$$
$$v(L) = 0 \tag{41}$$
$$w(L) = 0 \tag{42}$$
$$EI\Omega_n(L) = 0 \tag{43}$$
$$EI\Omega_b(L) = 0 \tag{44}$$

## Numerical Method

There are two differential variables in the governing equations of 3D dynamic subsea cable model: time variable $t$ and space variable $s$. The governing equations are highly nonlinear and strongly coupled. It is difficult to obtain analytical solutions except in simplified cases. The numerical method employed herein, is the Keller-Box finite difference approximation. The approximation begins with discretization of the cables into $n$ nodes and the governing equations are applied directly at each node. The governing partial differential equations of subsea cable problem are defined at $\left[i+\frac{1}{2}, k-\frac{1}{2}\right]$. The index $k$ define the nodes and the index $i$ define the time step.

$$\left.\frac{\partial \boldsymbol{Y}}{\partial t}\right|_{k-\frac{1}{2}}^{i+\frac{1}{2}} = \frac{\boldsymbol{Y}_k^{i+\frac{1}{2}}+\boldsymbol{Y}_{k-1}^{i+\frac{1}{2}}}{\Delta t} = \frac{1}{2}\left[\frac{\boldsymbol{Y}_k^{i+1}-\boldsymbol{Y}_k^{i}}{\Delta t}+\frac{\boldsymbol{Y}_{k-1}^{i+1}-\boldsymbol{Y}_{k-1}^{i}}{\Delta t}\right] \tag{45}$$

$$\left.\frac{\partial \boldsymbol{Y}}{\partial s}\right|_{k-\frac{1}{2}}^{i+\frac{1}{2}} = \frac{\boldsymbol{Y}_{k-\frac{1}{2}}^{i}+\boldsymbol{Y}_{k-\frac{1}{2}}^{i+1}}{\Delta t} = \frac{1}{2}\left[\frac{\boldsymbol{Y}_k^{i}-\boldsymbol{Y}_{k-1}^{i}}{\Delta s}+\frac{\boldsymbol{Y}_k^{i+1}-\boldsymbol{Y}_{k-1}^{i+1}}{\Delta s}\right] \tag{46}$$

where $\mathbf{Y} = [u \quad v \quad w \quad T \quad \phi \quad \theta \quad S_b \quad S_n \quad \Omega_n \quad \Omega_b]^{\mathrm{T}}$.

The entire lazy-wave subsea cable is divided into $n = n_l + n_b + n_u$ uniform elements. Touchdown catenary section, buoyancy catenary section and hang-off catenary section can be divided into $n_l, n_b$ and $n_u$ element respectively. These $10n$ nonlinear algebraic equations include $10n$ unknown parameters. At the static equilibrium state, the obtained parameters that calculated initially using the 3D static boundary conditions are set as parameters at time step $i = 1$. Then solved the next parameters at subsequent time step with suitable initial parameters using `fsolve` MATLAB built-in library of optimization program. The flowchart procedure on developing the MATLAB code is illustrated in Figure 4.

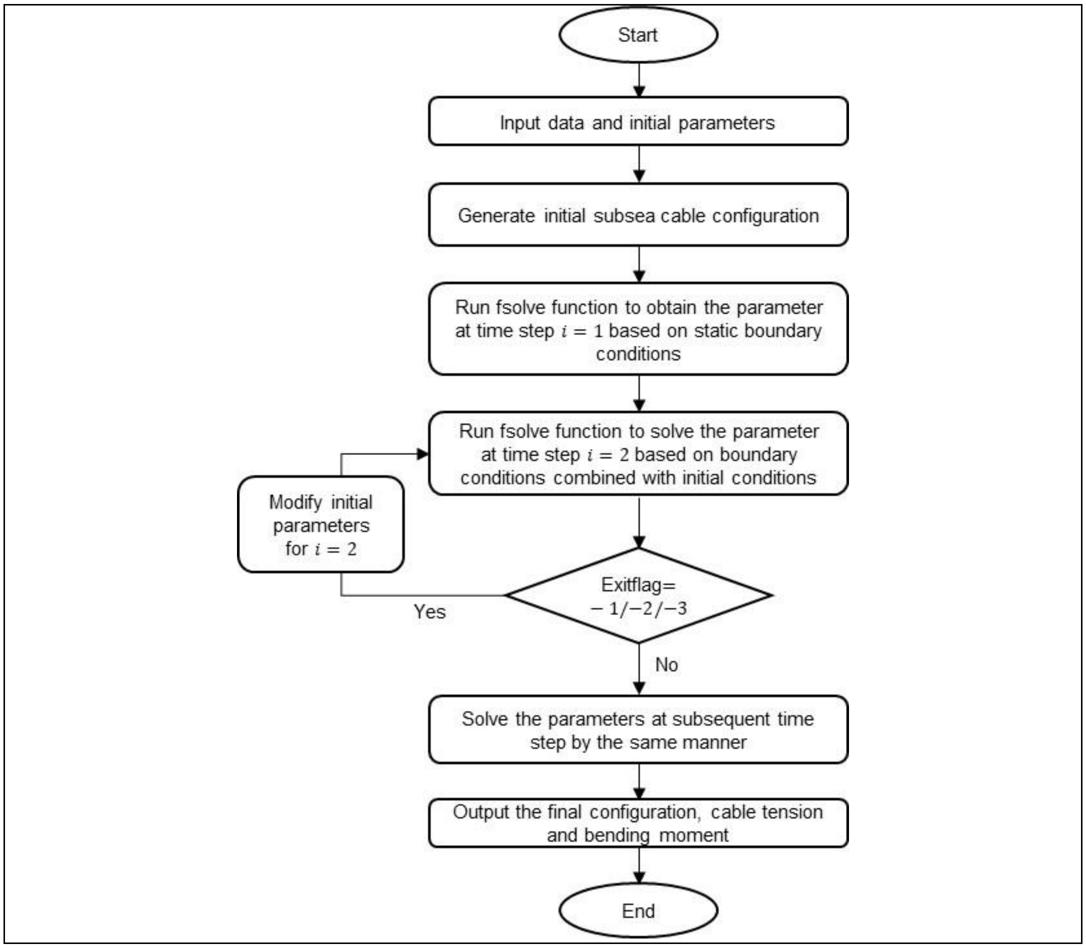


**Figure 4.** Flowchart of MATLAB procedure.

# Numerical Results and Discussion

## Comparison with Chatjigeorgiou [18]

To verify the reliability of the mathematical model of hang-off catenary cable, comparisons are performed with the results obtained from the proposed numerical method and results by Chatjigeorgiou [18]. He adopted a finite difference solution method to analyzed the dynamic cable problem. Both models presented here has same value of suspended length, $L = 2022\ \mathrm{m}$ and water depth, $h = 1800\ \mathrm{m}$. The input data used in the comparison is tabulated in Table 1.

**Table 1.** Input data for comparison (Subsea cable properties).

| Parameter | Value |
|---|---|
| Density of seawater, $\rho$ | $1024\ \mathrm{kg/m^3}$ |
| Outer diameter, $d_o$ | $0.429\ \mathrm{m}$ |
| Mass per unit length, $m_r$ | $262.933\ \mathrm{kg/m}$ |
| Added mass, $m_a$ | $148.16\ \mathrm{kg/m}$ |
| Wet weight per unit length, $w_r$ | $915.56\ \mathrm{N/m}$ |
| Axial stiffness, $EA$ | $0.5823 \times 10^{10}\ \mathrm{N}$ |
| Bending stiffness, $EI$ | $0.1209 \times 10^{9}\ \mathrm{Nm^2}$ |
| Tangential drag coefficient, $C_{dt}$ | $0.0$ |
| Normal drag coefficient, $C_{dn}$ | $1.0$ |

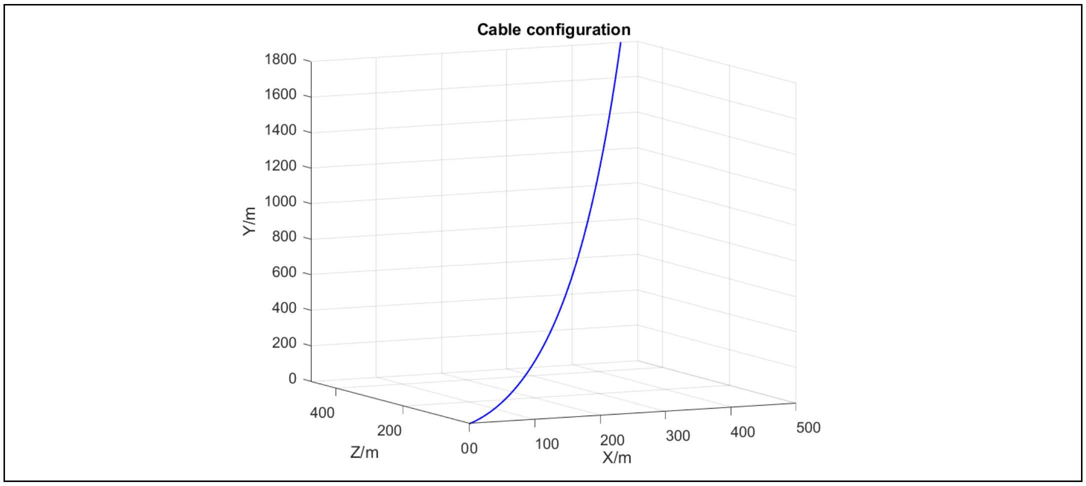


**Figure 5.** Configuration of the free-hanging cable for the 1800 m water depth.

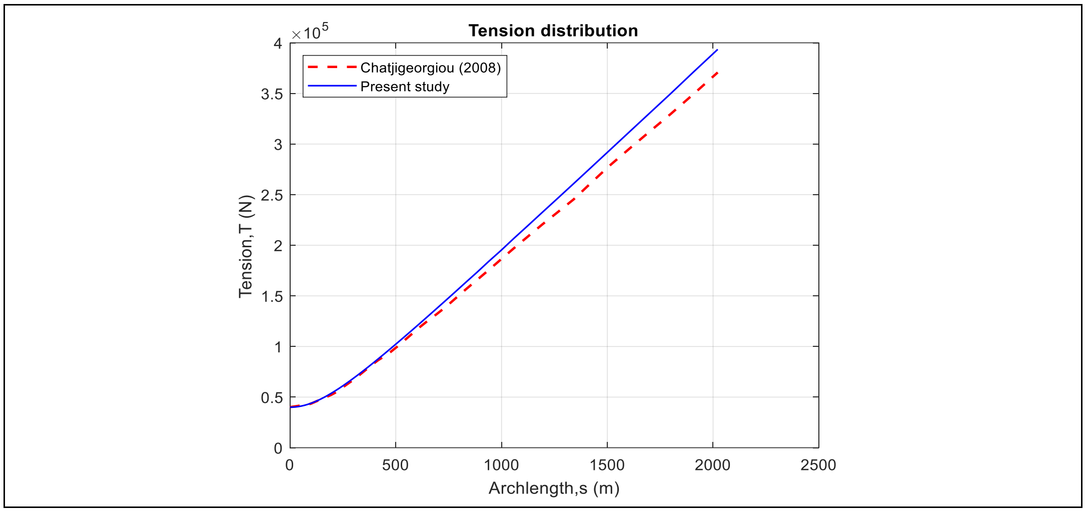


**Figure 6.** Tension distribution from the present model and Chatjigeorgiou [18].

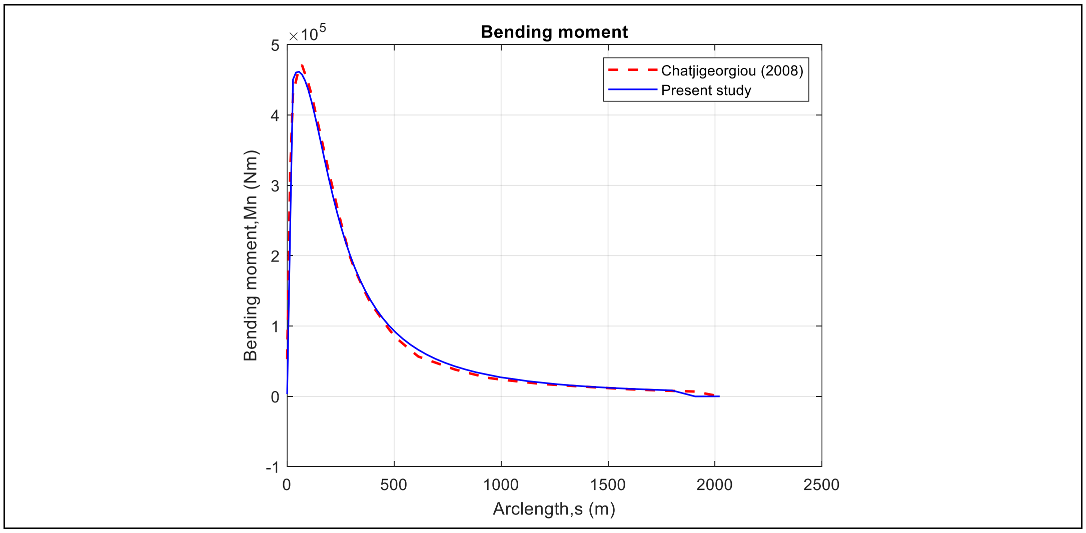


**Figure 7.** Bending moment from the present model and Chatjigeorgiou [18].

Based on the input data, cable tension and bending moment are calculated, and the results between the present study (solid line) and previous study (dash line) are shown in Figure 6 and 7. Figure 7 shows that the bending moment obtained from both models are almost identical. However, it is found in Figure 6 that the cable's tension distribution calculated form present theory is larger than that from Chatjigeorgiou [18] except for a small portion around the touchdown point surface. Tension distribution for both models is lower at the seabed and increase uniformly to a maximum value at the floating vessel. This is due to the gravitational effect in which the cable at the TDP is supported by seabed while the cable near hang-off point has to withstand the cable weight as there is no support.

## Numerical solutions

The numerical solution developed by using MATLAB program for both dynamic model of free-hanging cable and lazy-wave cable give the values of $u, v, w, T, \phi, \theta, S_b, S_n, \Omega_n$ and also $\Omega_b$. To have deeper insight into the subsea cable behaviour between free-hanging cable and lazy-wave cable, the effect of cable tension, and bending moment is studied here. The solution starts initially with calculating the static equilibrium position (the time items should be eliminated). Then, the static cable position will gradually evolve until it morphs into the optimal configuration/geometry with the existence of buoyancy module. For the lazy-wave cable, the equivalent submerged weight, $w_b$ is vertical upward with magnitude approximately equal to submerged weight of cable for the remaining sections, $w_b = -w_r$. The detailed physical properties used for the dynamic cable analysis with zero velocities of ocean current is tabulated in Table 2.

**Table 2.** Physical properties of subsea cable

| Parameter | Value |
|---|---|
| Density of seawater, $\rho$ | $1024\ \mathrm{kg/m^3}$ |
| Outer diameter, $d_o$ | $0.429\ \mathrm{m}$ |
| Mass per unit length, $m_r$ | $262.933\ \mathrm{kg/m}$ |
| Added mass, $m_a$ | $148.16\ \mathrm{kg/m}$ |
| Wet weight per unit length, $w_r$ | $915.56\ \mathrm{N/m}$ |
| Axial stiffness, $EA$ | $0.5823 \times 10^{10}\ \mathrm{N}$ |
| Bending stiffness, $EI$ | $0.1209 \times 10^{9}\ \mathrm{Nm^2}$ |
| Tangential drag coefficient, $C_{dt}$ | 0.0 |
| Normal drag coefficient, $C_{dn}$ | 1.0 |
| Pre-tension at TDP, $T_{TDP}$ | $150\ \mathrm{kN}$ |
| Touchdown catenary cable length, $S_l$ | $390\ \mathrm{m}$ |
| Buoyancy catenary cable length, $S_b$ | $520\ \mathrm{m}$ |
| Hang-off catenary cable length, $S_u$ | $1690\ \mathrm{m}$ |

### *3D cable configuration of free-hanging vs lazy-wave*

The cable configuration presented in this subsection, concern a cable which has a suspended length, $L = 2600\ \mathrm{m}$ and water depth, $h = 1650\ \mathrm{m}$. When we installed the buoyancy module to the middle section of free-hanging cable as illustrated in Figure 7, subsequently we will get a new configuration as Figure 8, namely lazy-wave subsea cable configuration. The red line from Figure 8 shows where the buoyancy module is installed. This buoyancy module created an upward buoyancy force which subsequently eliminate partial's cable tension distribution.

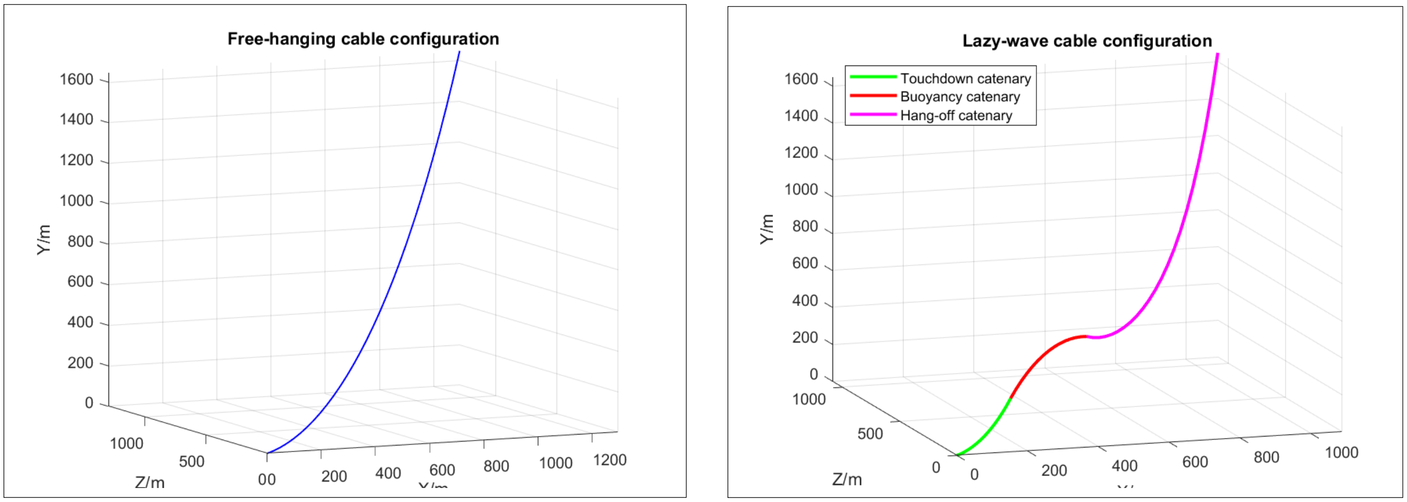


(a) (b)

**Figure 8.** Representation of subsea cable configuration obtained from MATLAB. (a) Free-hanging subsea cable. (b) Lazy-wave subsea cable

## Tension distribution and bending moment analysis

The numerical results, which are presented and discussed here, concern on the tension distribution and bending moment results from both free-hanging and lazy-wave cable. The objective is to reduce the formation of slack during the installation procedure. The initial hypothesis is that, when we implement the buoyancy module in the derivation of the model, the results will suggest a satisfactory cable configuration and a reduction in tension and bending moment along the subsea cable, hence, reduce the percentage of slacks and kinks due to the moving of cable ship.

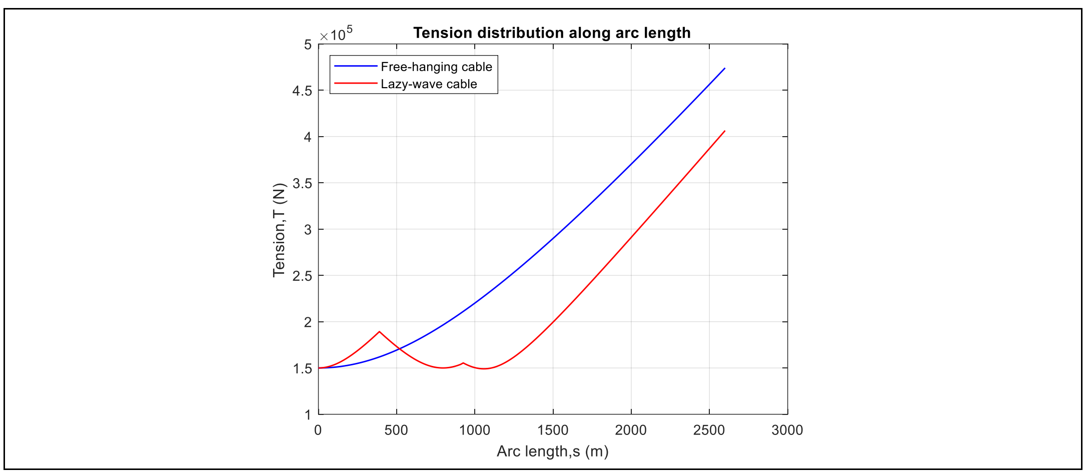


**Figure 9.** Tension distribution along arc length between free-hanging cable and lazy-wave cable.

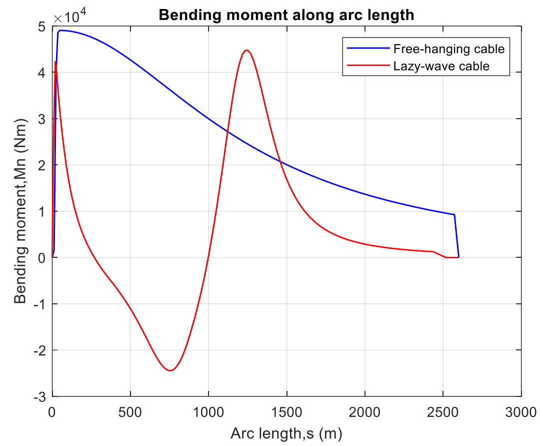


**Figure 10.** Bending moment along arc length between free-hanging cable and lazy-wave cable.

It can be seen clearly in tension distribution for lazy wave cable as shown in Figure 9 that the maximum tension distribution is around $(407\ k\mathrm{N})$ which is much smaller than maximum tension of free-hanging cable which the value is around $(474\ k\mathrm{N})$. This is an important advantage of installing the buoyancy module where it can reduce the top tension at the hang-off point. As shown in Figure 10, as there is no buoyancy catenary section in free-hanging cable, only one peak of the bending moment occurs along the subsea cable while there are two peaks for the lazy-wave cable. As a conclusion, from the MATLAB result, consequently lazy-wave cable can be considered as a good solution for deepwater problem since it produces much less cable tension compared to free-hanging cable.

## Effect of cable self-weight and pre-tension on the tension distribution

Cable self-weight and pre-tension are one of the key parameters to analyse the subsea cable behaviour during laying operations. Three different cable weight corresponding mass per unit length, weight of cable in air, and effective diameter of cable are considered in this example which is tabulated in Table 3 below. The pre-tension of cable at the TDP can be measured by tensiometer and it considered as a critical parameter during laying operation. A lower pre-tension at TDP can cause the cable to build loops or unwanted slack, while higher pre-tension will result in an exceedingly residual tension where it can cause detrimental effects on the cable. To ensure operation quality, it would best to adjust $T_{TDP}$ to an optimum value.

**Table 3.** Properties of cable self-weight

| **Parameter** | **Value** | | |
|---|---|---|---|
| | **Cable 1** | **Cable 2** | **Cable 3** |
| Outer diameter, $d_o$ | $0.08$ m | $0.10$ m | $0.11$ m |
| Mass per unit length, $m_r$ | $20$ kg/m | $30$ kg/m | $40$ kg/m |
| Weight per unit length, $w_r$ | $145.5$ N/m | $215.2$ N/m | $297.6$ N/m |
| Weight of cable in air | $196.12$ N/m | $294.18$ N/m | $392.24$ N/m |

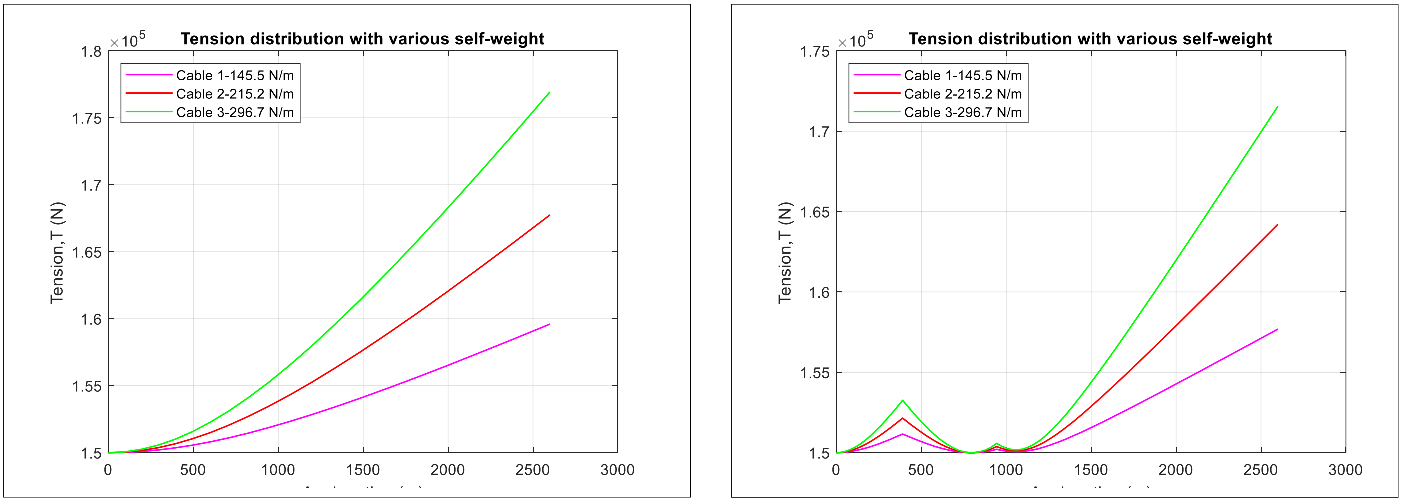


**(a)** **(b)**

**Figure 11.** Tension distribution with various self-weight. (a) Free-hanging (b) Lazy-wave cable.

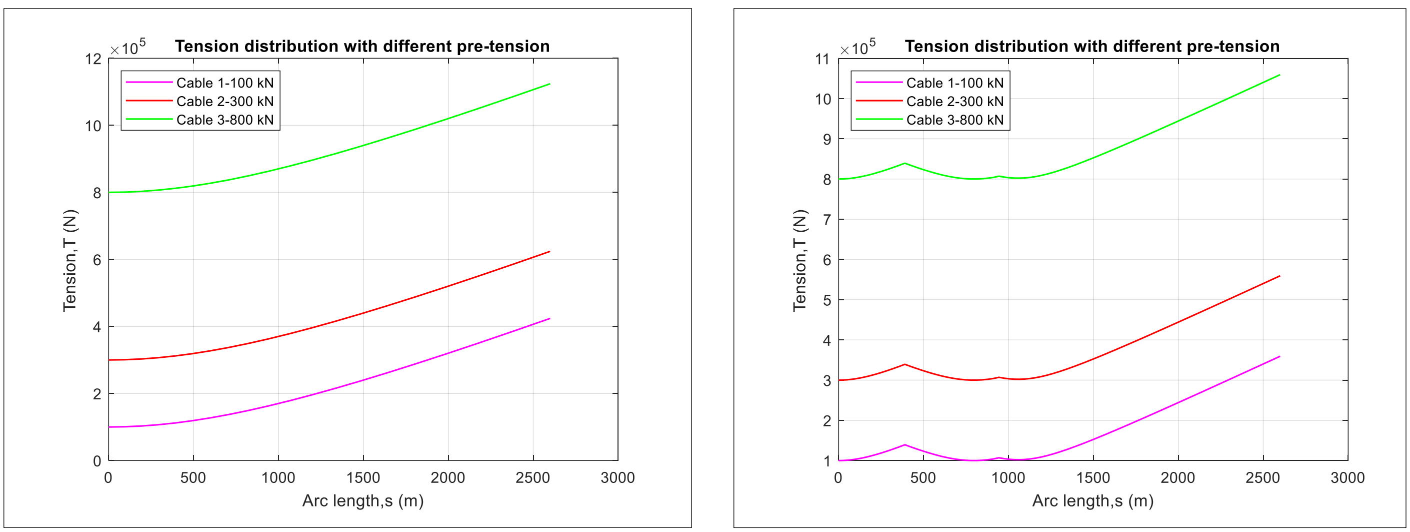


**(a)** **(b)**

**Figure 12.** Tension distribution with different pre-tension at TDP. (a) Free-hanging (b) Lazy-wave cable.

Result presented in Figure 11 shows that the influence of the cable self-weight per unit length on tension distribution is the difference of the tension becomes larger at the hang-off section as the arc length increases. Three cases of different pre-tension at TDP are illustrated in Figure 12, i.e., $T_{TDP} = 100\ \mathrm{kN}, 300\ \mathrm{kN}$ and $800\ \mathrm{kN}$. As shown in Figure 12, the difference in tension distribution between each pre-tension are increases linearly and consistent with each other.

## Conclusions

Subsea cables have been used for decades as a global communication and more recently internet services have grown in capacity around the world. Key to keep these developments is the exploration of more cable laying networks, especially in increasingly challenging areas, where a lot of new surroundings parameters may take place in the calculation. This study proposes a solution to some of these issues, particularly on controlling the wastage during the installation of subsea cables with buoyancy module. This is made possible by minimizing the potential slack and by synchronizing the movement of a ship/vessel with the suitable cable configuration. The maximum tension occurs at hang-off point which is critical parameter of cable laying operation. The lazy-wave cable configuration proved to be good alternative for deepwater than the free-hanging cable, as the buoyancy module reduce the maximum tension at the HOP in the free-hanging cable by at most 86%. In addition, the bending moment are at peak at a point near to TDP, so the mechanical loads at TDP must be paid special attention. Long-term investigation including deformation behavior and durability aspects of subsea cable and buoyancy module, however, has been put forward for future study to obtain better understanding of this subsea cable problem during the landing or laying operation.

## Conflicts of interest

The authors declare that there is no conflict of interest regarding the publication of this paper."

## Funding statement

The authors would like to express gratitude to the Ministry of Higher Education (MOHE) for the funding through the Fundamental Research Grant Scheme (FRGS) [FRGS Grant R.J130000.7854.5F194, Reference no: FRGS/1/2019/STG07/UTM/02/15].

## References

[1] Abidin, A. R. Z., *et al.* (2018). Subsea cable laying problem. *Matematika, 34*(2), 173-186.
[2] Vaz, M. and M. Patel. (2000).Three-dimensional behaviour of elastic marine cables in sheared currents. *Applied Ocean Research*, *22*(1), 45-53.
[3] Chucheepsakul, S. and N. Srinil. (2002). Free vibrations of three-dimensional extensible marine cables with specified top tension via a variational method. *Ocean Engineering*, *29*(9), 1067-1096.
[4] Han, H., X. Li, and H.-S. Zhou. (2018). 3D mathematical model and numerical simulation for laying marine cable along prescribed trajectory on seabed. *Applied Mathematical Modelling, 60*, 94-111.
[5] Wang, J., M. Duan, and J. Luo, (2015). Mathematical model of steel lazy-wave riser abandonment and recovery in deepwater. *Marine Structures, 41*, 127-153.
[6] Zargar, E. and M. Kimiaei. (2015). An investigation on existing nonlinear seabed models for riser-fluid-soil interaction studies in steel catenary risers. *Frontiers in Offshore Geotechnics III: Proceedings of the 3rd International Symposium on Frontiers in Offshore Geotechnics (ISFOG 2015)*. Taylor & Francis Books Ltd.
[7] Wang, J. and M. Duan. (2015). A nonlinear model for deepwater steel lazy-wave riser configuration with ocean current and internal flow. *Ocean Engineering*, *94*, 155-162.
[8] Katifeoglou, S.A. and I.K. Chatjigeorgiou. (2016). Dynamics of shell-like tubular segments at the sagbend region of a steel catenary riser. *Ships and Offshore Structures*, *11*(8), 860-873.
[9] Bai, X., *et al*. (2017). Dynamic tests in a steel catenary riser reduced scale model. *Ships and Offshore Structures*, *12*(8), 1064-1076.
[10] Kim, S. and M.-H. Kim. (2015). Dynamic behaviors of conventional SCR and lazy-wave SCR for FPSOs in deepwater. *Ocean Engineering*, *106*, 396-414.
[11] Wang, J., M. Duan, and R. He. (2018). A nonlinear dynamic model for 2D deepwater steel lazy-wave riser subjected to top–end imposed excitations. *Ships and Offshore Structures, 13*(3), 330-342.
[12] Trapper, P. A. (2020).Feasible numerical analysis of steel lazy-wave riser. *Ocean Engineering, 195,* 106643.
[13] Wang, J., *et al*. (2014). Numerical solutions for nonlinear large deformation behaviour of deepwater steel lazy-wave riser. *Ships and Offshore Structures, 9*(6), 655-668.
[14] Li, S. and C. Nguyen. (2010). Dynamic response of deepwater lazy-wave catenary riser. *Deep Offshore Technology International*, *147*.
[15] Oh, S., *et al*. (2019). dynamic simulation of steel lazy wave riser excited at the top-end. *The 29th International Ocean and Polar Engineering Conference*. OnePetro.
[16] Ai, S., *et al*. (2019). Performance comparison of stress-objective and fatigue-objective optimisation for steel lazy wave risers. *Ships and Offshore Structures*, *14*(6), 534-544.
[17] Cheng, Y., L. Tang, and T. Fan. (2020). Dynamic analysis of deepwater steel lazy wave riser with internal flow and seabed interaction using a nonlinear finite element method. *Ocean Engineering*, *209*, 107498.
[18] Chatjigeorgiou, I. K. (2008). A finite differences formulation for the linear and nonlinear dynamics of 2D catenary risers. *Ocean Engineering, 35*(7), 616-636.
[19] Hoffman, J. D. (1992). Numerical methods for engineers and scientists.
[20] Ablow, C. and S. Schechter. (1983). Numerical simulation of undersea cable dynamics. *Ocean Engineering*, *10*(6), 443-457.
[21] Milinazzo, F., M. Wilkie, and S. Latchman. 1987. An efficient algorithm for simulating the dynamics of towed cable systems. *Ocean Engineering*, *14*(6), 513-526.
[22] Chatjigeorgiou, I. K. (2010). Three dimensional nonlinear dynamics of submerged, extensible catenary pipes conveying fluid and subjected to end-imposed excitations. *International Journal of Non-Linear Mechanics*, *45*(7), 667-680.
[23] Chatjigeorgiou, I. K. and S. A. Mavrakos. (2010). The 3D nonlinear dynamics of catenary slender structures for marine applications. *Nonlinear Dynamics*. IntechOpen.